SCIENCE CHINA
Information Sciences

• **Supplementary File** •

Backstepping Control of a Quadrotor Unmanned Aerial Vehicle Based on Multi-rate Sampling

Fakui WANG[1], Weisheng CHEN[1], Hao DAI[1*], Jing LI[2] & Jinping JIA[2]

[1]*School of Aerospace Science and Technology , Xidian University, Xi'an* 710071*, China;*
[2]*School of Mathematics and Statistics, Xidian University, Xi'an* 710071*, China*

Appendix A Importance

Appendix A.0.1 *Dynamic model of quadrotor*

Ignoring the elastic deformation and vibration conditions, a quadrotor UAV can be regarded as a rigid body with six DOFs, and there are four rotors to generate the propeller forces F_1, F_2, F_3 and F_4. So the quadrotor UAV is a four-input and six-output control system. The six DOFs of the rigid body are the rotation of the three axes and the linear motion of the center of gravity along the three axes.

The dynamic model of the quadrotor UAV, shown in Figure $A1$, is established. There are two main coordinate systems (see the Figure A1): the earth-fixed intertial reference frame E^a: $(O^a,\vec{e_1^a},\vec{e_2^a},\vec{e_3^a})$ such that $\vec{e_3^a}$ represents a vertical upward direction, and the body-fixed reference frame E^m: $(O^m,\vec{e_1^m},\vec{e_2^m},\vec{e_3^m})$ fixed on the center of mass of the quadrotor UAV.

The rotation matrix from the body-fixed reference frame E^m to the earth-fixed intertial reference frame E^a is represented by $R_t \in \mathbb{R}^{3\times3}$ as follows:

$$R_t = \begin{bmatrix} C_\phi C_\psi & S_\phi S_\theta C_\psi - C_\phi S_\psi & C_\phi S_\theta C_\psi + S_\phi S_\psi \\ C_\theta S_\psi & S_\phi S_\theta S_\psi + C_\phi C_\psi & C_\phi S_\theta S_\psi - S_\phi C_\psi \\ -S_\phi & S_\phi C_\theta & C_\phi C_\theta \end{bmatrix}. \tag{A1}$$

The rotational angular velocity transfer matrix $R_r \in \mathbb{R}^{3\times3}$ is provided by

$$R_r = \begin{bmatrix} 1 & 0 & -S_\theta \\ 0 & C_\theta & C_\theta S_\phi \\ 0 & -S_\phi & C_\phi C_\theta \end{bmatrix}, \tag{A2}$$

where $C_{(\cdot)}$ and $S_{(\cdot)}$ represent $\cos(\cdot)$ and $\sin(\cdot)$, respectively.

Appendix A.0.2 *Backstepping controller design*

First, the altitude tracking errors are defined (the ground effect is ignored) as

$$e_i(t) = x_{id}(t) - x_i(t), \qquad i = 1, 3, ..., 11. \tag{A3}$$

We first consider about the virtual system $\dot{x_i} = v_i$ where $v_i(t)$ are virtual control input signals designed as follows

$$v_i = \dot{x}_{id} + \chi_i e_i, \quad \chi_i > 0. \tag{A4}$$

where χ_i are positive design constants.

The Lyapunov function candidates are chosen as $V(e_i) = \frac{1}{2}e_i^2$, and the time derivatives along (8) are

$$\dot{V}(e_i) = e_i\dot{e}_i = e_i(\dot{x}_{id} - v_i) = -\chi_i e_i^2 < 0. \tag{A5}$$

The speed tracking errors are

$$e_j(t) = v_i(t) - x_j(t), \qquad j = 2, 4, ..., 12, \tag{A6}$$

where $x_j = \dot{x_i}$.

* Corresponding author (email: dai0519hao@163.com)

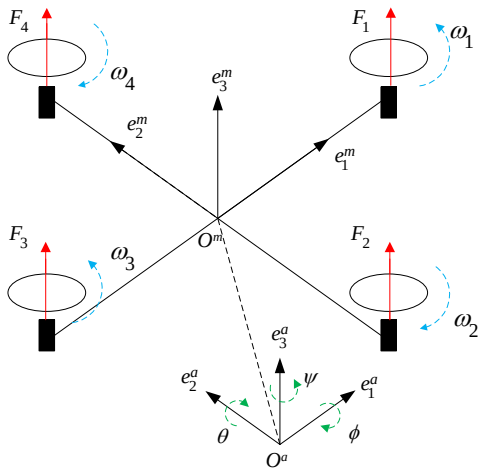

Figure A1 The earth-fixed intertial reference frame and the body-fixed reference frame.

The time derivatives of $e_i(t)$ can be written as

$$\dot{e}_i = \dot{x}_{id}(t) - \dot{x}_i(t) = -\chi_i e_i + e_j. \tag{A7}$$

Altitude control.

The altitude control law maintains the expected value of the helicopter to the ground.

The 2-order virtual system is considered as

$$\begin{cases} \dot{x}_5 = x_6, \\ \dot{x}_6 = (\cos x_7 \cos x_9)\dfrac{U_1}{m} - g. \end{cases} \tag{A8}$$

And U_1 is a control input signal to be designed as follows

$$U_1 = \frac{m}{\cos x_7 \cos x_9}(\ddot{x}_{5d} + e_5 + g + \chi_5(e_6 - \chi_5 e_5) + \tau_6 e_6), \tag{A9}$$

where τ_6 is a positive design constant.

We define a Lyapunov function as $V(e_5, e_6) = V(e_5) + \frac{1}{2}e_6^2$. Substitute (13) and (14) into the derivative of V, then we get

$$\begin{aligned} \dot{V}(e_5, e_6) &= e_5\dot{e}_5 + e_6\dot{e}_6 \\ &= e_5(-\chi_5 e_5 + e_6) + e_6(\ddot{x}_{5d} + \chi_5\dot{e}_5 - \dot{x}_6) \\ &= -\chi_5 e_5^2 + e_6(e_5 + \ddot{x}_{5d} + \chi_5(e_6 - \chi_5 e_5) + g - (\cos x_7 \cos x_9)\frac{U_1}{m}) \\ &= -\chi_5 e_5^2 - \tau_6 e_6^2 \\ &< 0. \end{aligned} \tag{A10}$$

Position control.

Position control law keeps the helicopter over the desired point.

The virtual system of x-axis is considered as

$$\begin{cases} \dot{x}_1 = x_2, \\ \dot{x}_2 = \dfrac{u_x}{m}U_1. \end{cases} \tag{A11}$$

u_x is a virtual control law to be designed as follows

$$u_x = \frac{m}{U_1}(\ddot{x}_{1d} + e_1 + \chi_1(e_2 - \chi_1 e_1) + \tau_2 e_2), \tag{A12}$$

where τ_2 is a positive design constant.

We define a Lyapunov function as $V(e_1, e_2) = V(e_1) + \frac{1}{2}e_2^2$. Substitute (16) and (17) into the derivative of V, then we get

$$\begin{aligned} \dot{V}(e_1, e_2) &= e_1\dot{e}_1 + e_2\dot{e}_2 \\ &= e_1(-\chi_1 e_1 + e_2) + e_2(\ddot{x}_{1d} + \chi_1\dot{e}_1 - \dot{x}_2) \\ &= -\chi_1 e_1^2 + e_2(e_1 + \ddot{x}_{1d} + \chi_1(e_2 - \chi_1 e_1) - \frac{u_x}{m}U_1) \\ &= -\chi_1 e_1^2 - \tau_2 e_2^2 \end{aligned}$$

$$< 0. \tag{A13}$$

Similarly, the virtual control law of y-axis is

$$u_y = \frac{m}{U_1}(\ddot{x}_{3d} + e_3 + \chi_3(e_4 - \chi_3 e_3) + \tau_4 e_4), \tag{A14}$$

where τ_4 is a positive design constant.

Attitude controller is the heart of the control system which keeps the 3D orientation of the helicopter to the desired value. The stability proof of control U_2, U_3, and U_4 are similar to U_1, so we won't do a detailed derivation here.

Appendix A.0.3 *Multi-rate sampling controller design*

For the **Theorem 1** in the letter, the first two terms of (6) are calculated as

$$U_{\lambda k0} = U_\lambda|_{t=k\delta},$$
$$U_{\lambda k1} = \dot{U}_\lambda|_{t=k\delta}.$$

The single-rate sampling controller is designed as follows

$$\begin{aligned}\widehat{U}_{1k} &= U_1|_{t=k\delta} + \frac{1}{2}\delta\dot{U}_1|_{t=k\delta} \\ &= \big[\frac{m}{\cos x_7 \cos x_9}(\ddot{x}_{5d} + e_5 + g + \chi_5(e_6 - \chi_5 e_5) + \tau_6 e_6) + \frac{\delta m}{2(\cos x_7 \cos x_9)^2}\big((\dddot{x}_{5d} + \dot{e}_5 + \chi_5(\dot{e}_6 - \chi_5\dot{e}_5) \\ &+ \tau_6\dot{e}_6)(\cos x_7 \cos x_9) + (\ddot{x}_{5d} + e_5 + g + \chi_5(e_6 - \chi_5 e_5) + \tau_6 e_6)(\dot{x}_7 \sin x_7 \cos x_9 + \dot{x}_9 \cos x_7 \sin x_9)\big)\big]_{t=k\delta},\end{aligned} \tag{A15}$$

$$\begin{aligned}\widehat{U}_{2k} &= U_2|_{t=k\delta} + \frac{1}{2}\delta\dot{U}_2|_{t=k\delta} \\ &= \big[\frac{1}{\beta_1}(\ddot{x}_{7d} + e_7 + \chi_7(e_8 - \chi_7 e_7) - x_{10}x_{12}\alpha_1 - x_{10}\alpha_2\Omega_r + \tau_8 e_8) + \frac{\delta}{2\beta_1}(\dddot{x}_{7d} + \dot{e}_7 + \chi_7(\dot{e}_8 - \chi_7\dot{e}_7) \\ &- \alpha_1(\dot{x}_{10}x_{12} + x_{10}\dot{x}_{12}) - \alpha_2(\dot{x}_{10}\Omega_r + x_{10}\dot{\Omega}_r) + \tau_8\dot{e}_8)\big]_{t=k\delta},\end{aligned} \tag{A16}$$

$$\begin{aligned}\widehat{U}_{3k} &= U_3|_{t=k\delta} + \frac{1}{2}\delta\dot{U}_3|_{t=k\delta} \\ &= \big[\frac{1}{\beta_2}(\ddot{x}_{9d} + e_9 + \chi_9(e_{10} - \chi_9 e_9) - x_8x_{12}\alpha_3 - x_8\alpha_4\Omega_r + \tau_{10}e_{10}) + \frac{\delta}{2\beta_2}(\dddot{x}_{9d} + \dot{e}_9 + \chi_9(\dot{e}_{10} - \chi_9\dot{e}_9) \\ &- \alpha_3(\dot{x}_8x_{12} + x_8\dot{x}_{12}) - \alpha_4(\dot{x}_8\Omega_r + x_8\dot{\Omega}_r) + \tau_{10}\dot{e}_{10})\big]_{t=k\delta},\end{aligned} \tag{A17}$$

$$\begin{aligned}\widehat{U}_{4k} &= U_4|_{t=k\delta} + \frac{1}{2}\delta\dot{U}_4|_{t=k\delta} \\ &= \big[\frac{1}{\beta_3}(\ddot{x}_{11d} + e_{11} + \chi_{11}(e_{12} - \chi_{11}e_{11}) - x_8x_{10}\alpha_5 + \tau_{12}e_{12}) + \frac{\delta}{2\beta_3}(\dddot{x}_{11d} + \dot{e}_{11} + \chi_{11}(\dot{e}_{12} - \chi_{11}\dot{e}_{11}) \\ &- \alpha_5(\dot{x}_8x_{10} + x_8\dot{x}_{10}) + \tau_{12}\dot{e}_{12})\big]_{t=k\delta}.\end{aligned} \tag{A18}$$

For the **Theorem 2** in the letter, the first two terms of (7) are calculated as

$$U^0_{\lambda 1k} = U_\lambda|_{t=k\delta},$$
$$U^0_{\lambda 2k} = U_\lambda|_{t=k\delta},$$
$$U^1_{\lambda 1k} = \frac{2}{3}\dot{U}_\lambda|_{t=k\delta},$$
$$U^1_{\lambda 2k} = \frac{10}{3}\dot{U}_\lambda|_{t=k\delta}.$$

The double-rate sampling controller is designed as follows

When $i = 1$, we can get $\widetilde{U}_{\lambda k} = U^0_{\lambda 1k} + \frac{1}{2}\bar{\delta}U^1_{\lambda 1k}$. Therefore, the results of the control laws are

$$\begin{aligned}\widetilde{U}_{1k} &= U_1|_{t=k\delta} + \frac{1}{6}\delta\dot{U}_1|_{t=k\delta} \\ &= \big[\frac{m}{\cos x_7 \cos x_9}(\ddot{x}_{5d} + e_5 + g + \chi_5(e_6 - \chi_5 e_5) + \tau_6 e_6) + \frac{\delta m}{6(\cos x_7 \cos x_9)^2}\big((\dddot{x}_{5d} + \dot{e}_5 + \chi_5(\dot{e}_6 - \chi_5\dot{e}_5) \\ &+ \tau_6\dot{e}_6)(\cos x_7 \cos x_9) + (\ddot{x}_{5d} + e_5 + g + \chi_5(e_6 - \chi_5 e_5) + \tau_6 e_6)(\dot{x}_7 \sin x_7 \cos x_9 + \dot{x}_9 \cos x_7 \sin x_9)\big)\big]_{t=k\delta},\end{aligned} \tag{A19}$$

$$\begin{aligned}\widetilde{U}_{2k} &= U_2|_{t=k\delta} + \frac{1}{6}\delta\dot{U}_2|_{t=k\delta} \\ &= \big[\frac{1}{\beta_1}(\ddot{x}_{7d} + e_7 + \chi_7(e_8 - \chi_7 e_7) - x_{10}x_{12}\alpha_1 - x_{10}\alpha_2\Omega_r + \tau_8 e_8) + \frac{\delta}{6\beta_1}(\dddot{x}_{7d} + \dot{e}_7 + \chi_7(\dot{e}_8 - \chi_7\dot{e}_7) \\ &- \alpha_1(\dot{x}_{10}x_{12} + x_{10}\dot{x}_{12}) - \alpha_2(\dot{x}_{10}\Omega_r + x_{10}\dot{\Omega}_r) + \tau_8\dot{e}_8)\big]_{t=k\delta},\end{aligned} \tag{A20}$$

Parameters	Value	Unit
m	2.2	kg
l	0.275	m
I_x	6.23×10^{-3}	$kg \cdot m^2$
I_y	6.23×10^{-3}	$kg \cdot m^2$
I_z	1.12×10^{-2}	$kg \cdot m^2$
J_r	1.54×10^{-5}	$kg \cdot m^2$
k_1	3.13×10^{-5}	/
k_2	7.45×10^{-7}	/

Table A1 Parameters of the quadrotor model

$$\begin{aligned}\widetilde{U}_{3k} &= U_3|_{t=k\delta} + \frac{1}{6}\delta\dot{U}_3|_{t=k\delta} \\ &= \big[\frac{1}{\beta_2}(\ddot{x}_{9d} + e_9 + \chi_9(e_{10} - \chi_9 e_9) - x_8 x_{12}\alpha_3 - x_8\alpha_4\Omega_r + \tau_{10}e_{10}) + \frac{\delta}{6\beta_2}(\dddot{x}_{9d} + \dot{e}_9 + \chi_9(\dot{e}_{10} - \chi_9\dot{e}_9) \\ &\quad - \alpha_3(\dot{x}_8 x_{12} + x_8\dot{x}_{12}) - \alpha_4(\dot{x}_8\Omega_r + x_8\dot{\Omega}_r) + \tau_{10}\dot{e}_{10})\big]_{t=k\delta}, \end{aligned} \tag{A21}$$

$$\begin{aligned}\widetilde{U}_{4k} &= U_4|_{t=k\delta} + \frac{1}{6}\delta\dot{U}_4|_{t=k\delta} \\ &= \big[\frac{1}{\beta_3}(\ddot{x}_{11d} + e_{11} + \chi_{11}(e_{12} - \chi_{11}e_{11}) - x_8 x_{10}\alpha_5 + \tau_{12}e_{12}) + \frac{\delta}{6\beta_3}(\dddot{x}_{11d} + \dot{e}_{11} + \chi_{11}(\dot{e}_{12} - \chi_{11}\dot{e}_{11}) \\ &\quad - \alpha_5(\dot{x}_8 x_{10} + x_8\dot{x}_{10}) + \tau_{12}\dot{e}_{12})\big]_{t=k\delta}. \end{aligned} \tag{A22}$$

When $i = 2$, we can draw $\widetilde{U}_{\lambda k} = U^0_{\lambda 2k} + \frac{1}{2}\overline{\delta}U^1_{\lambda 2k}$. Hence, the control laws are respectively computed as

$$\begin{aligned}\widetilde{U}_{1k} &= U_1|_{t=k\delta} + \frac{5}{6}\delta\dot{U}_1|_{t=k\delta} \\ &= \big[\frac{m}{\cos x_7 \cos x_9}(\ddot{x}_{5d} + e_5 + g + \chi_5(e_6 - \chi_5 e_5) + \tau_6 e_6) + \frac{5\delta m}{6(\cos x_7 \cos x_9)^2}\big((\dddot{x}_{5d} + \dot{e}_5 + \tau_5(\dot{e}_6 - \chi_5\dot{e}_5) \\ &\quad + \tau_6\dot{e}_6)(\cos x_7 \cos x_9) + (\ddot{x}_{5d} + e_5 + g + \chi_5(e_6 - \chi_5 e_5) + \tau_6 e_6)(\dot{x}_7 \sin x_7 \cos x_9 + \dot{x}_9 \cos x_7 \sin x_9)\big)\big]_{t=k\delta}, \end{aligned} \tag{A23}$$

$$\begin{aligned}\widetilde{U}_{2k} &= U_2|_{t=k\delta} + \frac{5}{6}\delta\dot{U}_2|_{t=k\delta} \\ &= \big[\frac{1}{5\beta_1}(\ddot{x}_{7d} + e_7 + \chi_7(e_8 - \chi_7 e_7) - x_{10}x_{12}\alpha_1 - x_{10}\alpha_2\Omega_r + \tau_8 e_8) + \frac{\delta}{6\beta_1}(\dddot{x}_{7d} + \dot{e}_7 + \chi_7(\dot{e}_8 - \chi_7\dot{e}_7) \\ &\quad - \alpha_1(\dot{x}_{10}x_{12} + x_{10}\dot{x}_{12}) - \alpha_2(\dot{x}_{10}\Omega_r + x_{10}\dot{\Omega}_r) + \tau_8\dot{e}_8)\big]_{t=k\delta}, \end{aligned} \tag{A24}$$

$$\begin{aligned}\widetilde{U}_{3k} &= U_3|_{t=k\delta} + \frac{5}{6}\delta\dot{U}_3|_{t=k\delta} \\ &= \big[\frac{1}{5\beta_2}(\ddot{x}_{9d} + e_9 + \chi_9(e_{10} - \chi_9 e_9) - x_8 x_{12}\alpha_3 - x_8\alpha_4\Omega_r + \tau_{10}e_{10}) + \frac{\delta}{6\beta_2}(\dddot{x}_{9d} + \dot{e}_9 + \chi_9(\dot{e}_{10} - \chi_9\dot{e}_9) \\ &\quad - \alpha_3(\dot{x}_8 x_{12} + x_8\dot{x}_{12}) - \alpha_4(\dot{x}_8\Omega_r + x_8\dot{\Omega}_r) + \tau_{10}\dot{e}_{10})\big]_{t=k\delta}, \end{aligned} \tag{A25}$$

$$\begin{aligned}\widetilde{U}_{4k} &= U_4|_{t=k\delta} + \frac{5}{6}\delta\dot{U}_4|_{t=k\delta} \\ &= \big[\frac{1}{5\beta_3}(\ddot{x}_{11d} + e_{11} + \chi_{11}(e_{12} - \chi_{11}e_{11}) - x_8 x_{10}\alpha_5 + \tau_{12}e_{12}) + \frac{\delta}{6\beta_3}(\dddot{x}_{11d} + \dot{e}_{11} + \chi_{11}(\dot{e}_{12} - \chi_{11}\dot{e}_{11}) \\ &\quad - \alpha_5(\dot{x}_8 x_{10} + x_8\dot{x}_{10}) + \tau_{12}\dot{e}_{12})\big]_{t=k\delta}. \end{aligned} \tag{A26}$$

Appendix A.0.4 *Comparison and verification*

The parameters of the quadrotor UAV used in the simulations are shown in Table $A1$.

Assuming that the quadrotor moves from the origin $(x, y, z) = (0, 0, 0)$ of the ground coordinate system E^a to the target point $(x, y, z) = (2, 2, 2)$, the yaw angle ψ moves from 0 to $0.1rad$, and the initial states of the roll angle ϕ and pitch angle θ are 0.

Figure.$A2$ shows the states of motion of the quadrotor under a continuous-time controller. As we can see, the space motion of the quadrotor is stabilized at the target value $(2, 2, 2)$ after a period of adjustment. And the attitude angle of the quadrotor has reached a steady state after adjustment for a period of time. The yaw angle ψ is steady at $0.1rad$, and

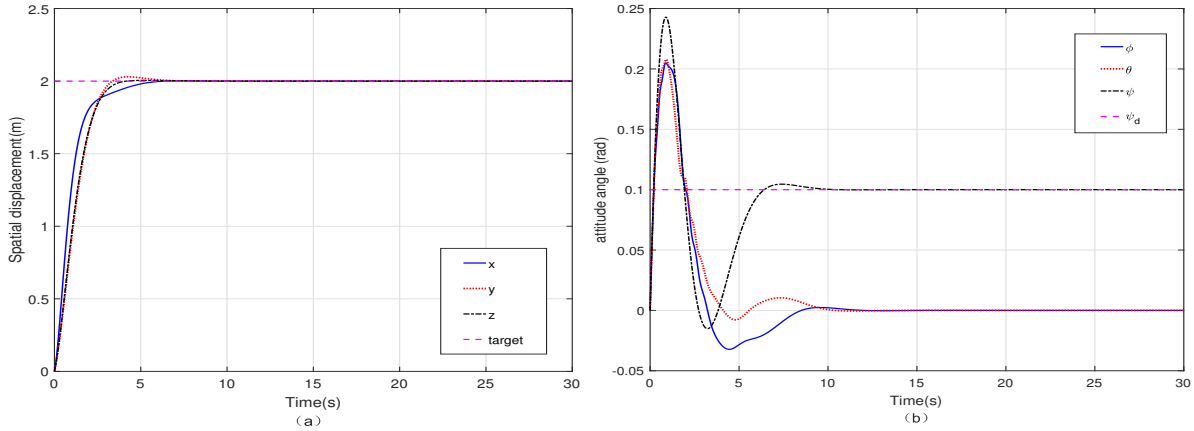

Figure A2 The states of motion of the quadrotor under a continuous-time controller, (a) represents the spatial displacement, (b) represents the attitude angle.

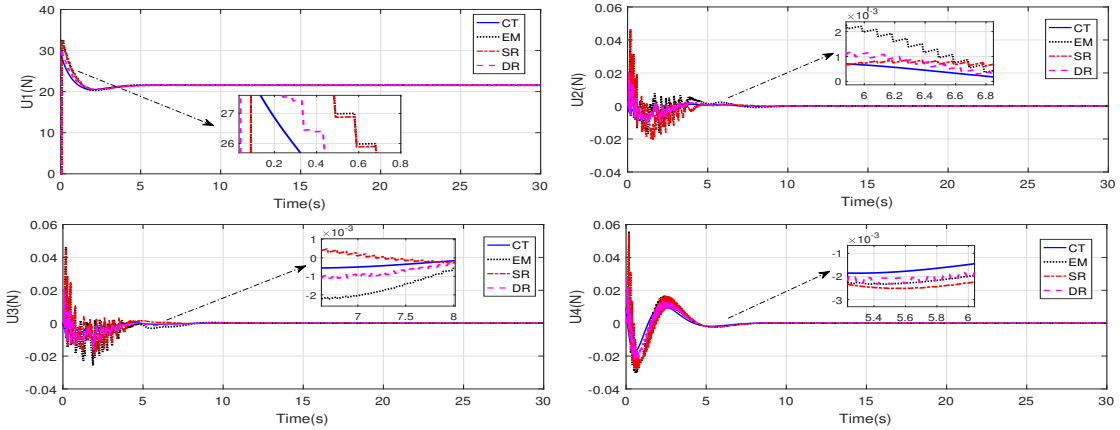

Figure A3 The comparison of control inputs between multi-rate sampling controllers and continuous-time controller during the sampling period $\delta = 0.01$.

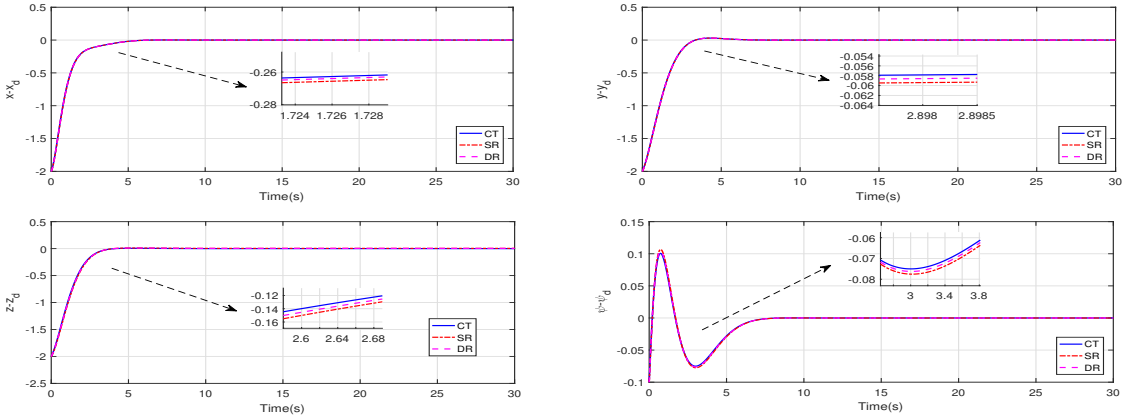

Figure A4 Error comparison between single-rate sampling controller and multi-rate sampling controller when sampling time is $\delta = 0.01$.

the roll angle ϕ and pitch angle θ are steady at 0. Figure A3 shows the comparison of the control inputs between the multi-rate sampling controller and the continuous-time controller during the sampling period $\delta = 0.01$. We can see that the system under single-rate sampling controller and double-rate sampling controller have also stabilized after a period of time. From these simulations, we can see that all the digital control strategies perform well when the sampling period δ is smaller. We can see from figure $A4$ that the curve of multi-rate sampling controller is closer to that of continuous-time

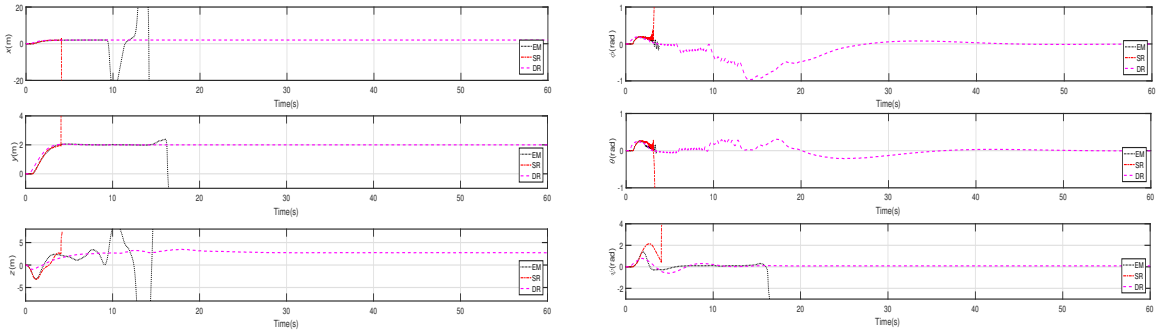

Figure A5 The state curve of UAV at $\delta = 0.80$

controller than that of single-rate sampling controller. Therefore, the control precision of multi-rate sampling control is higher than that of single-rate sampling controller. Figure.$A5$ shows that, with a large sampling period $\delta = 0.80$, the double-rate sampling controller still achieved stabilization and presented an acceptable performance, while the emulated and the single-rate controller cannot guarantee stability anymore.

Remark 1. Compared with the single-rate sampling controller, the multi-rate sampling controller adds more control inputs in one sampling period. Their sampling period is the same. But the multi-rate sampling controller calculates the controller multiple times in each sampling period.